Journal of **A**pplied **B**iotechnology **R**eports

Original Article

Electrochemical Behavior of Adult and Fetal Hemoglobin at Gold-coated Magnetic Iron Oxide Nanoparticle

Khadijeh Eskandari[1], Hedayatollah Ghourchian[2], Aghdas Banaei[3*]

Abstract

A feasible and fast method for Adult Hemoglobin (A-Hb) and Fetal Hemoglobin (F-Hb) study was developed by immobilization of Hb on gold-coated magnetic iron oxide nanoparticles (GMNPs).The prepared GMNPs composite nanoparticles with 60 nm diameter were used as a carrier for the immobilization of Hb. The A-Hb and F-Hb were physically attached to the GMNPs nanoparticles. The direct electrochemistry of F-Hb and A-Hb showed a quasi-reversible cyclic voltammogram corresponding to the Heme group with a formal potential of 314 and -334 mV in 0.1M PBS (pH 6.2), respectively. The apparent charge transfer rate constant (ks) and transfer coefficient (α) for electron transfer between the electrode surface and protein were calculated as 0.29/s and 0.1 for F-Hb and 0.21/s and 0.47 for A-Hb. The linear concentration rangesare17.3–225 and 7.4-53 mM for F-H band A-Hb biosensors for H_2O_2detection. The lifetime of biosensor is more than 2 weeks.

1. Nanobiotechnology Research Center, Baqiyatallah University of Medical Sciences, Tehran, Iran
2. Laboratory of Microanalysis, Institute of Biochemistry and Biophysics, University of Tehran, Tehran, Iran
3. Research Institute of Applied Science, Academic Center of Education, Culture and Research (ACECR), Shahid Beheshti University, Tehran, Iran

*** Corresponding Author**
Aghdas Banaei
Research Institute of Applied Science, Academic Center of Education, Culture and Research (ACECR), ShahidBeheshti University, Tehran, Iran
E-mail: a_banaei@ut.ac.ir

Submission Date: 5/24/2017
Accepted Date: 6/28/2017

Keywords: Biosensor, Direct Electrochemistry, H_2O_2, Gold-coated, Iron Oxide Nanoparticles, Hemoglobin

Introduction

Hemoglobin (Hb) is one of important redox proteins with four electroactiveiron hemes and a molar mass of approximately67 kDa [1]. Electrochemical study of Hb has been describedin a many of publications, for great importance of hydrogen peroxide (H_2O_2) determination in food, pharmaceutical, clinical, industrial, environmental analysis and many other fields. Hb has commonly been employed to make H2O2 biosensors for its commercial availability and peroxidase activity. Also, electrochemical methods, such as amperometric,for their simplicity, high selectivity and good sensitivity, have been extensively employed. Therefore, too many Hb electrochemical biosensors were developed every year. However, electron transfer between redox proteins and bare solid electrodes is usually slow and it is facilitated by variety immobilization strategies such as hydrogel polymer, surfactants and nanomaterials [2].

As a voluble nanomaterial, metal nanoparticles for their advantage such as; unique electronic, optical, and catalytic properties due to the quantum size effects are highly attended [3]. The gold nanoparticles exhibit many attractive properties in the application to H_2O_2biosensors because of their highly conducting material, good biocompatibility and simple synthetic procedure [4].

On the other hand, nowadays the magnetic nanoparticles receive increasing attention in designing electrochemical enzyme biosensors [5-6]. Magnetic nanoparticles as the immobilization platforms have some advantages such as: few fouling, selective and fast separation of the immobilized proteins from the reaction mixture by the application of a magnetic field, high conductivity and immobilization of enzyme on electrode without the need for any chemical linker or electrode modification by magnetic force [7-9]. GMNPs nanoparticles are a very attractive nano-composite with synergetic properties that leads to the improvement in the biosensor performance. The biosensors based on GMNPs nanoparticles display interesting electrochemical and biocompatible properties due to Au and magnetic properties of Fe_3O_4.

In this work, A-Hb and F-Hb immobilized on GMNPs nanocomposite and used as a conductive platform for constructing H_2O_2 electrochemical biosensor using cyclic voltammetery (CVs) and chronoamperometry modes. Also, the kinetics and analytical parameters of biosensor based on A-Hb and F-Hb were compared.

Materials and Methods

Materials

A-Hb and F-Hb were extracted and purified from human red blood cells of healthy donors and umbilical cord blood of newborn respectively .H_2O_2 were purchased from Sigma and used as received. $FeCl_2{\cdot}7H_2O$, $FeCl_3{\cdot}6H_2O$, NaOH, HCl, tetramethyl-ammonium hydroxide pentahydrate ($TMAOH.5H_2O$) were purchased from Sigma–Aldrich (Steinheim, Germany). Chloroauric acid trihydrate ($HAuCl_4{\cdot}\ 3H_2O$), potassium trisodium citrate, potassium dihydrogen phosphate (KH_2PO_4) and potassium hydrogen phosphate (K_2HPO_4) were purchased from Merck and used

as delivered. The solutions were prepared in deionized double distilled water (18 MΩ.cm, Barnstead, Dubuque, USA) and all experiments were carried out at room temperature (25°C).

Apparatus and measurements

All electrochemical experiments were performed with potentiostat/galvanostat (model 263-A, EG&G, USA) controlled by a Power Suite software package and a GPIB interface. Electrochemical studies were performed using a single-compartment conventional three-electrode cell (volume 300 µl). A gold-disk working electrode with a diameter of 2 mm equipped with a permanent magnet under it, a saturated silver/silver chloride (Ag/AgCl) reference electrode, containing 3 M KCl (from Azar electrode, Iran), and a platinum rod auxiliary electrode were used. All potentials were measured and reported versus the Ag/AgCl reference electrode. The morphology of the synthesized GMNPs nanoparticles was obtained using a SEM Model LEO 440i, UK. TheUV-Vis spectra were carried out using a Cary spectrophotometer, 100 Bio-model. (Japan). The electrochemical behavior of Hb and detection of H_2O_2 was carried out in an air-saturated solution for similarity of *in vivo* usage.

Preparation of adult and fetal hemoglobin

A-Hb was prepared from human red blood cells of healthy donors as reported in our previous study [10]. Briefly, the heparinized blood was first centrifuged to remove plasma components. Then, the packed red cells were washed three times in an isotonic saline solution (0.9 % NaCl) and cosmetically lysed with cold double distilled water. Membrane components were removed by low-speed centrifugation (3,000 rpm). The Hb solution was then brought to 20 % saturation with ammonium sulfate, kept for about 15 min, and centrifuged at 20,000 rpm for 1 h at 2°C. The supernatant containing A-Hb were dialyzed at least three times in PBS (50 mM, pH 7.4) for 24 h. Fetal hemoglobin was prepared from umbilical cord blood of newborn using the same procedure as that mentioned for A-Hb.

Preparation of the gold-coated iron oxide nanoparticle (GMNPs)

The GMNPs was prepared by the procedures described in literature [11]. In short, 5.4 g $FeCl_2 \cdot 7H_2O$ and 2.0 g $FeCl3 \cdot 6H_2O$ were dissolved in 25 ml of 10 mM HCl and the solution was added drop wise to 250 ml of 1.5 M NaOH solution under vigorous stirring. A black precipitate was immediately formed. It was washed with distilled water to remove the NaOH excess and heated at 60°C to dryness. In order to encapsulate the iron nanoparticles with the gold shells, 5mL of iron oxide nanoparticles suspended in 0.1M TMAOH solution (pH 12) was added to 95 ml of citric acid (5 mM) and stirred vigorously. Finally, 0.2 M $NH_2OH \cdot HCl$ and 1% $HAuCl_4 \cdot 3H_2O$ were alternatively added into the magnetite solution until the solution became purple.

Electrode preparation

GMNPs nanoparticles were equilibrated in phosphate buffer (0.1 M, pH 6.2), and transferred on the gold plate electrode surface and were fixed using a permanent magnet. Then, 5 µl (10 mg/ml) solution of Hb dropped on GMNPs. During this step, Hb reacted with the GMNPs, giving rise to physically bonds. Then, to remove the additional and loosely bound Hb molecules, it washed with the PBS three times. The prepared electrode was stored at 4°C before use.

Results and discussion

UV-Vis Spectroscopy and SEM characterization of synthesized GMNPs nanoparticles

The UV–Vis absorption spectra of iron oxide nanoparticles (a), Au nanoparticles (b) as reference samples and GMNPs nanoparticles (c) were observed in Fig. 1. The black magnetic nanoparticle do not show absorption peaks in UV–Vis spectrum (a). Red color gold colloid and GMNPs colloid with a black-red color exhibit an absorption band with maxima at 526 and 538nm, respectively. The result confirms the gold coating of the iron oxide nanoparticles in spectrum (c). Furthermore, spectrum (c) is broader than spectrum (b). The red shift and broadening in the surface plasmon absorption of the GMNPs colloid relative to the pure Au colloid reveals that the size distribution of pure Au nanoparticles is narrower than that of the GMNPs nanoparticles and the aggregation of GMNPs nanoparticles is more than the pure Au nanoparticles [12]. Also, Fig. 2 shows the SEM images of GMNPs in spherical shape and their average diameter is around 50 nm.

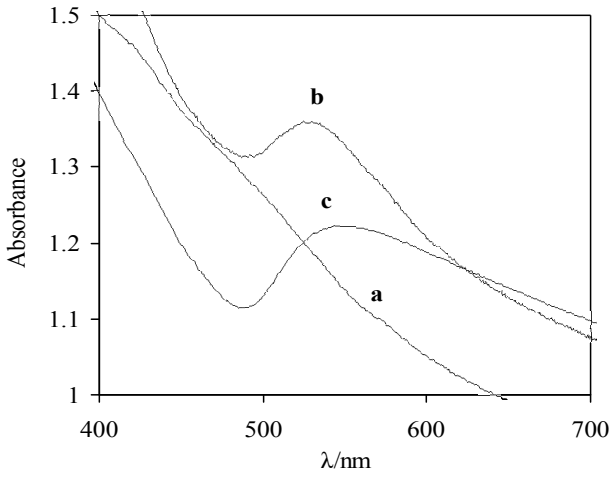

Figure 1. UV–Vis absorption spectra of (a) Fe_3O_4NPs, (b) GNPs and (c) GMNPs.

Electrochemical properties of Hb on GMNPselectrode

The direct electrochemistry of F-Hb and A-Hb immobilized on GMNPs/Au electrode was investigated using CV. Figure 3 shows the CVs of the GMNPs/Au electrode (a), F-Hb/GMNPs/Au electrode (b) and A-Hb/GMNPs/Au electrode (c) respectively, in 0.1 M PBS (pH 6.2) and air-saturated condition. Curve (a) revealed that, the GMNPs/Au electrode did not show any response. However, it was obvious that the modified electrode exhibited excellent and quasi-reversible redox peaks, as shown in curve (b) and (c). The formal potential (E0) has been calculated by average of the cathodic and anodic potentialsthat are -314 and -334 mV (vs. Ag/AgCl) with the potentials separation of 308 and 219 mV for F-Hb and A-Hb, respectively. This result suggests that most of the

Hb molecules preserved their native structure after the attachment on magnetic nanoparticles.

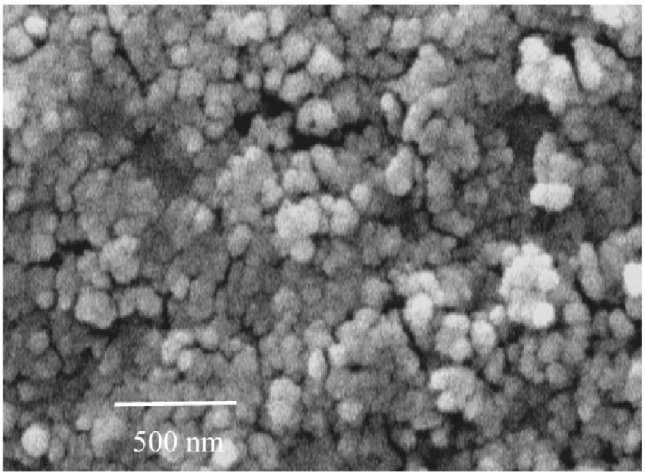

Figure 2. SEM image of GMNPs.

Nonetheless, in comparison between F-Hb and A-Hb, it is obvious that, by immobilization of F-Hb on the GMNPs electrodes, it is more susceptible to aggregation for irreversible CVs peak.

Figure 4A and 5A show the cyclic voltammograms of F-Hb/GMNPs/Au and A-Hb/GMNPs/Au electrode in PBS (0.1 M, pH 6.2) at different scan rates. Figure 4B and 5B show the plot of cathodic and anodic peaks current (I_p) against the scan rate (υ). Both the anodic and cathodic peak currents increased linearly with square scan rate in the region of 5-500 mV/s indicating surface controlled redox reaction, as expected for immobilized systems [13].

The kinetic parameters of electron transfer coefficient (α) and apparent charge transfer rate constant (k_s) can be calculated using Laviron's model [14].

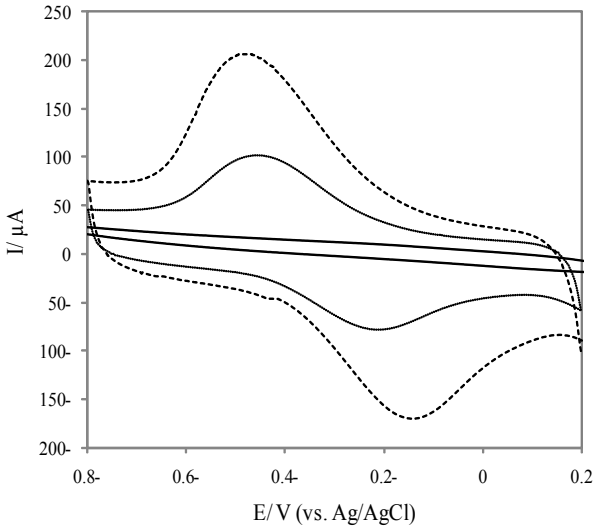

Figure 3. CVs of GMNPs/Au (Solid line), AHb/GMNPs/Au (Dotted line) and FHb/GMNPs/Au electrodes (Dashed line), in air-saturated PBS (0.1 M, pH 6.2). The scan rate was 50 mV/s.

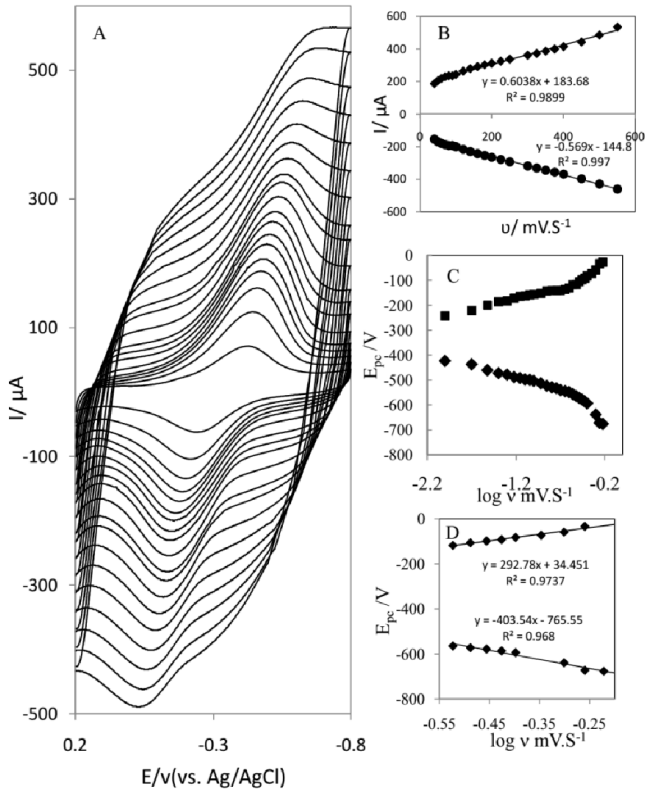

Figure 4. (A) CVs of FHb/GMNPs/Au electrode in PBS (0.1 M, pH 6.2) at various scan rates of 10, 20, 30, 40,60, 100, 140, 160, 200, 250, 300, 325, 350, 375, 400, 450, 500, 550 and 600 mV/s (vs. Ag/AgCl) from inner to outer, respectively, (B) plot of I_p vs ν, (C) plot of E_p vs. log ν and (D) plot of E_{pa} (Up) and E_{pc}(Down) vs log ν.

Laviron derived general expressions for the linear potential sweep voltammetric response for the case of surface-confined electroactive species at small concentrations (Eqs. (1) - (4)):

$$E_{pc} = E^0 + \frac{RT}{(1-\alpha)nF} \ln\left[\frac{(1-\alpha)}{m}\right] \quad (1)$$

$$E_{pa} = E^0 + \frac{RT}{(1-\alpha)nF} \ln\left[\frac{(\alpha)}{m}\right] \quad (2)$$

$$E_{pa} - E_{pc} = \Delta E_p > \frac{200}{n}\, mV \quad (3)$$

$$K_s = \alpha \log(1-\alpha) + (1-\alpha)\log\alpha - \log\left(\frac{RT}{nFv}\right) - \frac{\alpha(1-\alpha)nF\,\Delta E_p}{2.3RT} \quad (4)$$

where m= (RT/F)(k_s/nυ), k_s is the apparent charge transfer rate constant, αis the charge transfer coefficient, n is the number of electrons transferred in the rate-determining reaction, ΔE_p is the peak potential separation; R, T, and F have their usual meanings (R = 8.314 J/mol.K, T= 298 K,

F=96483 C/mol) and υ is the scan rate. α can be calculated using the plot of peak potentials (E_p) vs. logarithm of scan rate (logυ).

The slope of the linear section in cathodic and anodic peaks in Fig. 4C and 5C are equal to $-2.303RT/\alpha_c F$ and $2.303RT/\alpha_a nF$, respectively. As seen in Fig. 4D and 5D, it was found that for scan rates above 200 mV/s, $\Delta E = E_p - E^{o\prime}$ was proportional to the logυ, as indicated by Laviron. Therefore, we extracted the average value of 0.29 and 0.1/s for α and k_s, respectively for F-Hb/GMNPs/Au electrode. Also, α and k_s were extracted in the average value of 0.21 and 0.47/s for A-Hb/GMNPs/Au electrode.

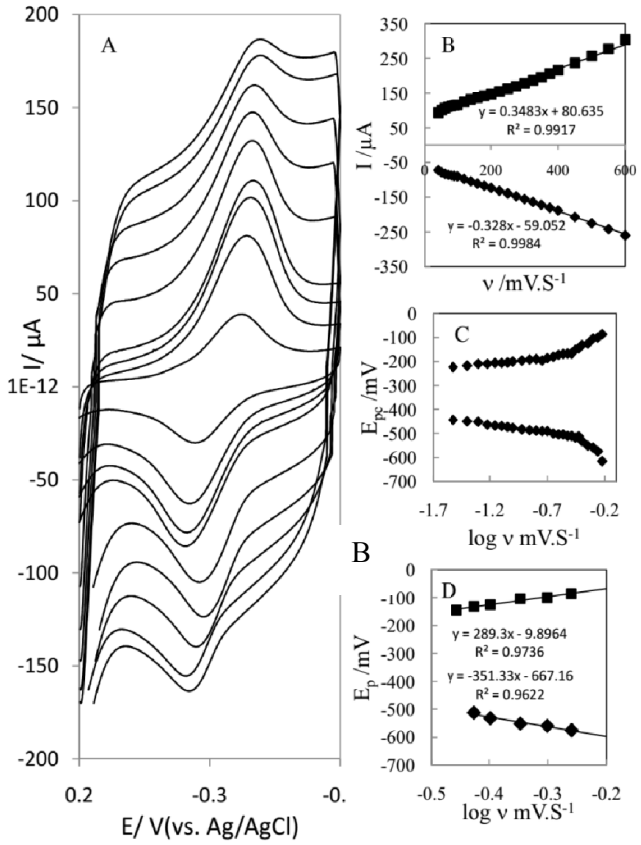

Figure 5. (A) CVs of AHb/GMNPs/Au electrode in PBS (0.1 M, pH 6.2) at various scan rates of 20, 30, 50, 70, 100, 150, 200, 250 and 300 mV/s (vs. Ag/AgCl) from inner to outer, respectively, (B) plot of I_p vs ν, (C) plot of E_p vs. log ν and (D) plot of E_{pa} (Up) and E_{pc} (Down) vs log ν.

Effect of pH on the peak potential

The voltammetric behavior of the F-Hb and A-HbGMNPs/Au electrodes were investigated at various pH by CV in Fig.6 and Fig. 7, respectively. These show peak-currents of the electrode in PBS at various pHs ranging from 5.8 to 8. As seen in Fig. 6B and Fig. 7B, the cathodic peak current rose with pH change from 5.8 to 6.2 and then decreased from pH 6.2 to 7.8. The maximum cathodic current was obtained at pH 6.2, therefore it was chosen as the optimal pH for further experiments.

As illustrated in Fig. 6A and Fig. 7A, the formal potential (E^0) of F-Hb and A-HbGMNPs/Au electrodes would beli-

nearly pH dependent. An increase in solution pH caused a negative shift in both cathodic and anodic peak potentials. The results showed that the slope (E^o/pH) is 66 and 57 mV/pH (for F-Hb and A-Hb, respectively) over a pH range from 5.8 to 7.8. This slope was close to the Nernstian value of 59.2 mV for a one-electron, one-proton process [15].

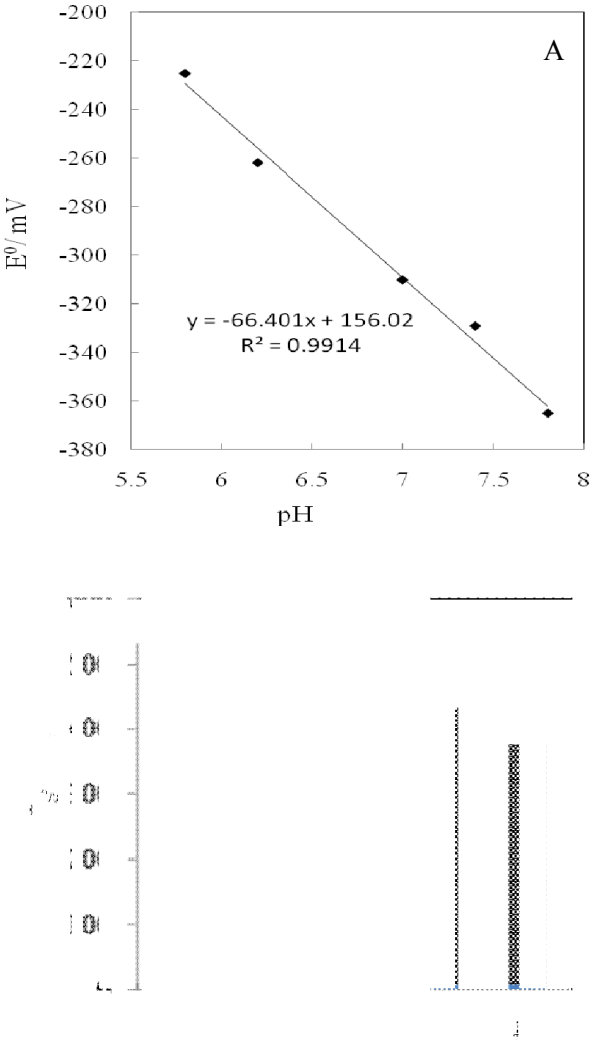

Figure 6. The plot of E^o vs. pH (A) and I_{pc} vs. pH (B) for FHb/GMNPs/Au electrode in 0.1 M PBS at different pHs. The scan rate was 50 mV/s (vs. Ag/AgCl).

Determination of $H_2O_2$by chronoamperometry

Figure 8 A and B compares the electrocatalytic reduction of hydrogen peroxide at both F-Hb and A-Hb GMNPs/Au electrodes, respectively. Subsequent addition of H_2O_2 to the solution resulted in an increase in the reduction current. The linear concentration range of F-Hb/GMNPs/Au biosensor was17.3–225 mM with detection limit of 12mM at S/N = 3 (with the regression equation of: y = 4.545x + 129.5, R^2 = 0.99). The linear concentration range of A-Hb/SMNPs/Au biosensor was 7.4-53 mM with detection limit of 7 mM at S/N = 3 (with the regression equation of: y = 0.816x + 24.26 R^2 = 0.99).

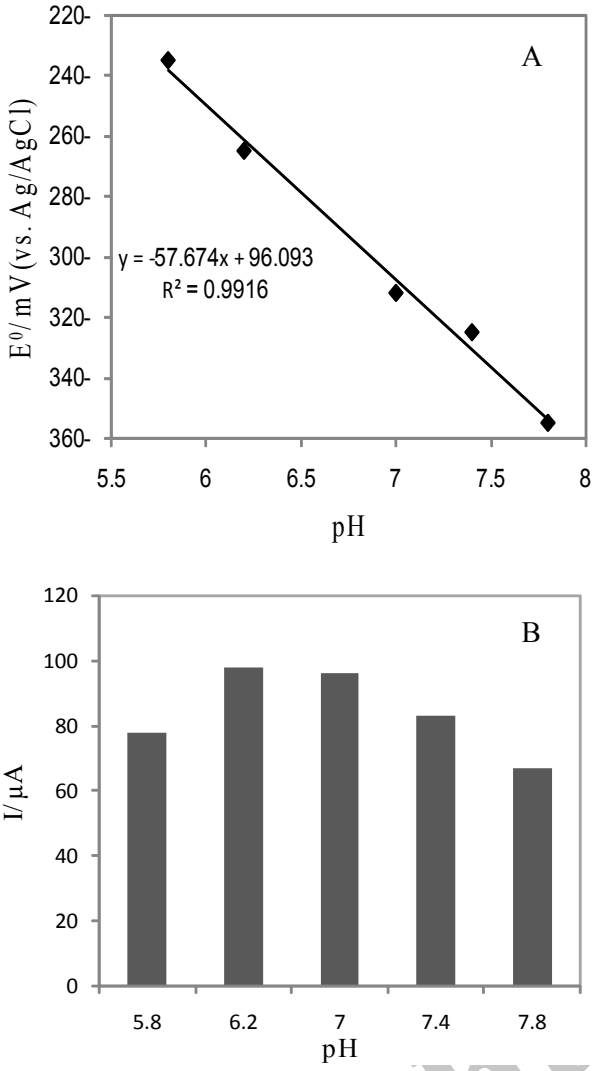

Figure 7. The plot of I_{pc} vs. pH (A) and E^o vs. pH (B) for Hb/GMNPs/Au electrode in 0.1 M PBS at different pHs. The scan rate was 50 mV/s (vs. Ag/AgCl).

Table 1. Comparison of electrochemical and electroanalytical parameters of A-Hb and F-Hb on modified electrodes.

No.	E^0 (V)	ΔE (V)	α	K_s/s	Linear range (mM)	DL (mM)
A-Hb	-0.334	0.219	0.21	0.47	7.4-53	7
F-Hb	-0.314	0.308	0.29	0.1	17.3–225	12

Finally, the analytical parameters of these biosensors were compared with other similar sensors reported for determination of H_2O_2 (Table 1). F-Hb biosensor based on the GMNPs electrodes shows a strong density electron transferring, due to aggregation and exposing of Hem groups on electrode surface. So, F-Hb biosensor is good candidate for H_2O_2 detection in comparable with A-Hb.

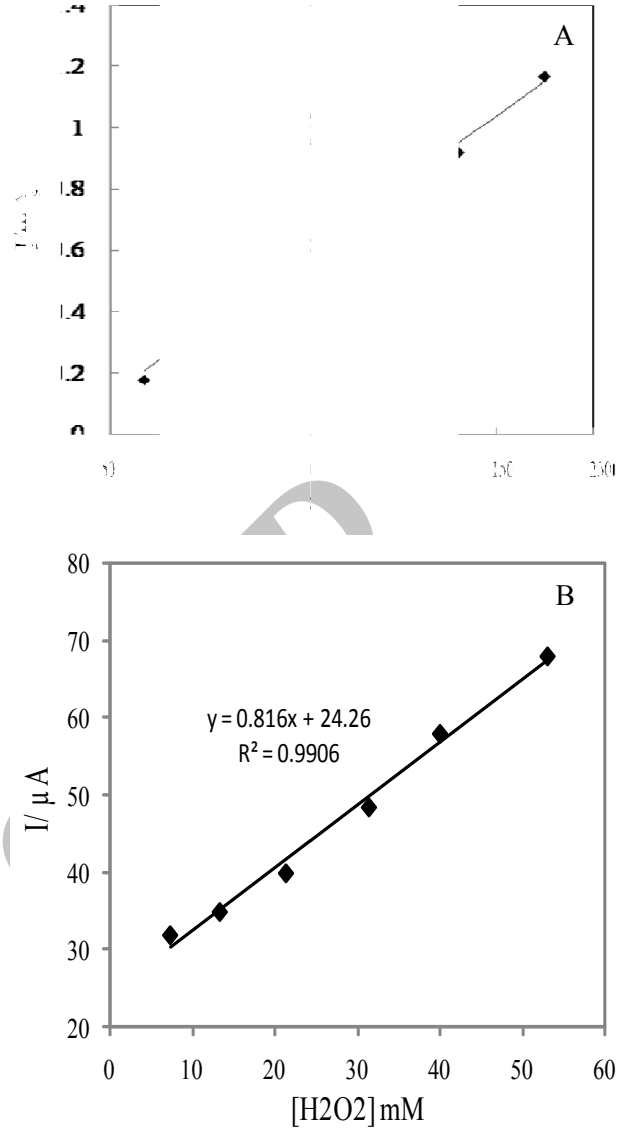

Figure 8. Calibration curve for the H_2O_2 in F-Hb/GMNPs/Au (A) and A-Hb/GMNPs/Au electrode (B) by chronoamperometry in 0.1 M pH 6.2 PBS containing various concentrations of H_2O_2 at the air-saturated conditions.

Conclusion

Due to the application of noble metal nanoparticles for development of miniaturized electronic devices such as biosensors, biocompatibility of these nanoparticles is important. Nanoparticles can absorb proteins via electrostatic interaction and/or covalent bonds formed between the gold or silver atoms and either amine groups of lysine residues or thiol groups of cysteine residues. The F-Hb and A-Hb immobilized on the GMNPs electrodes exhibit a direct and quasi-reversible electrochemical reaction. The results demonstrate that, although F-Hb immobilized on the GMNPs electrodes shows a strong electron density transferring, but it is more susceptible to aggregation by having irreversible CVs peaks. So, we propose F-Hb biosensor due to wide linear rang for analytical application and A-Hb biosensor for kinetic study.

Acknowledgements
The support provided by Research Council of the Baqiyatallah University of Medical Sciences, is gratefully acknowledged.

References

1. Liu, S., Dai, Z., Chen, H.,Ju, H., Immobilization of hemoglobin on zirconium dioxide nanoparticles for preparation of a novel hydrogen peroxide biosensor. *Biosens Bioelectron*, 2004, Vol. 19, pp. 963-969.
2. Lai, G., Zhang, H., Han, D., A novel hydrogen peroxide biosensor based on hemoglobin immobilized on magnetic chitosan microspheres modified electrode. *Sens Actuat B*, 2008, Vol. 129, pp. 497-503.
3. Sun, W., Sun, Z., Zhang, L., Qi, X., Li, G., Wu, J., Wang, M., Application of Fe_3O_4 mesoporous sphere modified carbon ionic liquid electrode as electrochemical hemoglobin biosensor colloid. *Surf B: Biointerf*, 2013, Vol. 101, pp. 177-182.
4. Mah-Heidari, N., Rashidiani, J., Dashtestani, F., Taheri, R., Sedighian, H.,Eskandari, Comparing signal amplification of thiocyanated Gold nanoparticles in the presence of different ions. *Int J Bio Inorg Hybr Nanomater*, 2017, Vol. 7, pp. 105-111.
5. Zhang, S., Wang, N., Niu, Y., Sun, C., Immobilization of glucose oxidase on gold nanoparticles modified Au electrode for the construction of biosensor. *Sens Actuat B*, 2005, Vol. 109,pp. 367-374.
6. Rashidiani, J., Moosavi, J., Eskandari, K., Ebrahimi, F., Novel free label botulinum aptasensor based on capacitance method. *St Cerc St CICBIA*, 2016, Vol. 17, pp. 169-178.
7. Huang, H., Liu, X., Zhang, X., Liu, W., Su, X., Zhang, Z., Fabrication of new magnetic nanoparticles (Fe_3O_4) grafted multiwall carbon nanotubes and heterocyclic compound modified electrode for electrochemical sensor. *Electroanal*, 2010, Vol. 22, pp. 433-442.
8. Chen, D., Liao, M., Preparation and characterization of YADH-bound magnetic nanoparticles. *Mol J Catal B*, 2002, Vol. 16, pp. 283-291.
9. Zarei, H., Ghourchian, H., Eskandari, K., Zeinali, M.,Magnetic nanocomposite of anti-human IgG/COOH–multiwalled carbon-nanotubes/Fe_3O_4 as a platform for electrochemical immunoassay. *Anal Biochem*, 2012, Vol. 421, pp. 446-453.
10. Banaei, A., Ghourchian, H., Rahimi, P., Moosavi-Movahedi, A-A., Amjadi, R., Different electrochemical behavior of adult and fetal hemoglobin at ionic liquid-carbon nanotube nanocomposite. *J Iran Chem Soc*, 2015, Vol. 12, pp. 687-694.
11. Pham, T. T. H., Cao, C., Sim. S. J., Application of citrate-stabilized gold-coated ferric oxide composite nanoparticles for biological separations. *J Magnet Magnet Mater*, 2008, Vol. 320, pp. 2049-2055.
12. Eskandari, K., Ghourchian, H.,Structural changes of glucose oxidase upon interaction with gold-coatedmagnetic nano-particles. *Inter J Biol Macromol*, 2012, Vol. 51, pp. 998-1002.
13. Rahimi, P., Rafiee-Pour, H. A., Ghourchian, H., Norouzi, P., Ganjali, M.R., Ionic-liquid/NH_2-MWCNTs as a highly sensitive nano-composite for catalase direct electrochemistry. *Biosens Bioelectron*, 2010, Vol. 25, pp. 1301-1306.
14. Shourian, M., Ghourchian, H., Biosensing improvement of horseradish peroxidase towards hydrogen peroxide upon modifying the accessible lysines. *Sens Actuat B*, 2010, Vol. 145, pp. 607-612.
15. Eskandari, K., Zarei, H., Ghourchian, H., Amoozadeh, M.,The Electrochemical study of glucose oxidase on gold coated magnetic iron oxide nanoparticles. *J Anal Chem*, 2015, Vol**.** 70, pp. 1254-1260.